Preparation, Characterization, and Anti-Anemia Activity Study of Polygonatum Polysaccharide-Iron(III) Complex

Mingming Han[1],Juan Pei[1],Sijin Tao[1],Shengxin Cui[1] ,Teng Peng[1,*]

[1] College of Pharmacy, Chengdu University of TCM, Chengdu 611137, China;
Mingmingh1999@outlook.com(M.H.);1636832739@qq.com(J.P.);1911865348@qq.com(S.T.);cuilingxin@yeah.net(S.C.)

***** Correspondence:pengteng1973@sina.com

Abstract

Iron deficiency anemia (IDA) is one of the most common nutritional deficiencies in the world. In this study, the polysaccharide (PSP) was purified from Polygonati Rhizoma by water extraction and alcohol precipitation, DEAE-52 anion exchange chromatography, Sephadex G100 and dialysis. The polysaccharide-iron complex (PSP-Fe) was synthesized by heating with $FeCl_3$. The physical and chemical properties and structure of the complex were characterized by SEM-EDS, FT-IR, XRD, TG, CD and UV, and its thermal stability was analyzed. In addition, the anti-IDA activity of the complex was verified by pharmacological experiments. The results showed that the iron content of the polysaccharide-iron complex was about 20.31%. The microstructure analysis showed that the polysaccharide-iron complex had a sheet-like morphology with a smooth and dense surface. In addition, the formation of Fe^{3+} complex did not change the structural skeleton of polysaccharides, but improved the thermal stability of polysaccharides. Pharmacological results showed that the compound had a good improvement effect on IDA rats. Therefore, the new compound shows significant potential as a viable iron supplement.

Keywords: Polygonatum Polysaccharide, Polysaccharide-iron (III) complex, Structural characterization, Iron deficiency anemia

1. Introduction

Polygonatum species are widely distributed globally and have a long history of medicinal use. Research indicates that polysaccharides are one of the primary active components in Polygonatum, exhibiting diverse biological activities and health benefits. Furthermore, in the Chinese Pharmacopoeia, polysaccharides have been

established as evaluation markers for quality control of medicinal materials such as Polygonatum[1]. Zhao et al.[2]revealed that the content and composition of polysaccharides were important features to distinguish different Polygonati Rhizoma.At least five types of polysaccharides have been identified in Polygonatum, including fructan [3], pectin[4], glucogalactomannan[5], glucomannan[6], and arabinogalactan-type polysaccharides[7]. Among these, pectin and fructan are the most frequently reported polysaccharides in PSP. On the other hand, PSP has been reported to exhibit osteogenic activity anti-obesity effects[8],anti-diabetic properties[9],antioxidant activity[10], antidepressant effects[11], and anti-aging effects [12].

Iron is one of the most important trace elements in the human body, essential for normal physiological functions, particularly as a cofactor in metabolism and immune function [13]. Iron deficiency anemia (IDA) is a nutritional deficiency disorder primarily associated with chronic inadequate iron intake, rapid iron loss, or impaired gastrointestinal absorption. In severe cases, IDA can lead to immunosuppression, pallor, dizziness, fatigue, and other adverse effects. A World Health Organization report estimates [14]that 46% of children aged 5–14 and 48% of pregnant women worldwide suffer from anemia, with most cases attributable to iron deficiency[15]. Oral iron supplementation is clearly essential for treating and preventing iron deficiency in humans[16]. However, oral iron supplements like ferrous salts commonly cause upper abdominal pain, diarrhea, and constipation severe enough to necessitate treatment discontinuation[13][17][18].Conversely,when iron intake exceeds requirements, supplements may become biologically toxic. Thus, developing novel iron supplements with minimal or no side effects is imperative[19][20].

Recent studies indicate that iron(III) complexes exhibit good bioavailability, with biocompatibility comparable to that of commonly used ferrous sulfate supplements. Among iron(III) complexes, polysaccharide-iron complexes have been most extensively studied due to their stability, water solubility, and reduced side effects [21][22]. Polysaccharide iron complexes prevent hydrolysis and dissolve metals, providing a non-toxic form of relatively high iron concentrations under physiological conditions. These complexes can serve as iron supplements for treating iron deficiency anemia (IDA) [23]

2. Materials and Methods

2.1. Materials

Polygonatum sibiricum Red. is produced in Yanshou County, Qiqihar City, Heilongjiang Province(**Figure 1**), and has been identified as the botanical source.DEAE-52, Sephadex G-100, and monosaccharide reference standards were obtained from Beijing Ruida Henghui. All other reagents were of analytical grade.

Figure 1. The aerial parts and rhizomes of Polygonatum. (A) Aerial part, (B) Rhizome

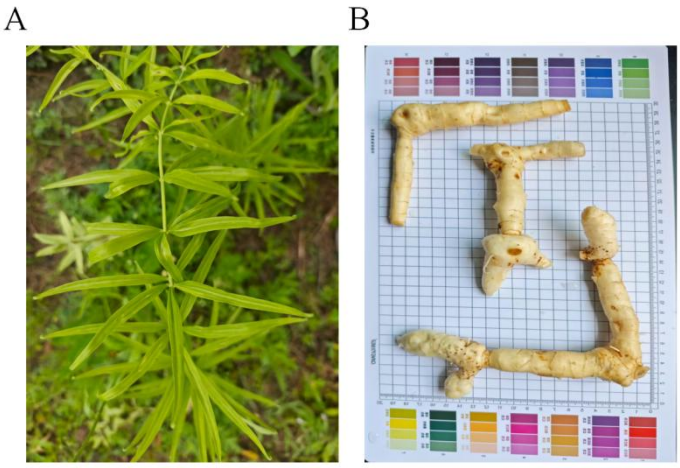

2.2.Extraction, Separation, and Purification of Polygonatum Polysaccharides

Fresh Polygonatum rhizomes were washed, air-dried, sliced, and dried in a 60°C oven to constant weight. After degreasing with petroleum ether and removing small-molecule impurities with 80% ethanol, the material underwent two 10-fold water extractions. Filtrates were combined and concentrated to a specific volume. Add anhydrous ethanol to achieve ethanol concentrations of 40%, 60%, and 80%, yielding three crude polysaccharide precipitates. Based on yield and solubility comparisons, the 80% ethanol fraction was selected for further study. Purification was achieved through protein removal with Sevage reagent, DEAE-52 anion exchange chromatography, G100 dextran gel filtration, and dialysis.

2.3.Preparation of PSP-Fe Complexes

The method for preparing polysaccharide complexes was adapted from Liu[24] and Zhang[25] et al. with minor modifications.Place an appropriate amount of PSP and sodium citrate into a beaker, dissolve with an adequate volume of deionized water, and slowly add 2 mol/L $FeCl_3 \cdot 6H_2O$ while stirring continuously. Adjust the solution pH to 8–9 using 2 mol/L HCl or 2 mol/L NaOH, then react at 70°C for 1 hour. After

the reaction, centrifuge the mixture at 4000 r/min for 15 min. Remove the lower precipitate layer, concentrate the supernatant, and dialysize it in distilled water to remove unbound iron ions. Finally, concentrate the dialysate, precipitate it with anhydrous ethanol, centrifuge, and freeze-dry to obtain the Polygonatum polysaccharide-iron(III) complex. This compound is designated PSP-Fe(III).

2.5.Structural Characterization Analysis

2.5.1.Chemical Composition Analysis

Iron content was determined using the o-phenanthroline method, with ammonium iron sulfate as the standard material for plotting the calibration curve. Total polysaccharide content was measured using the anthrone sulfuric acid method.

2.5.2.UV and FTIR analysis

Ultraviolet measurements were performed using a Shimadzu UV2600i spectrophotometer, while FT-IR spectroscopy (Thermo Fisher iS5) was employed to investigate the vibrational spectra of various atomic bonds and polar bonds. PSP and PSP-Fe(III) complexes were weighed and mixed with dry KBr in a 150:1 ratio. The mixture was then ground into fine particles and compressed into pellets. Scanning was performed over the wavelength range of 4000 to 400 cm^{-1}.

2.5.3.Scanning electron microscopy (SEM)

Surface microstructures of polysaccharides and polysaccharide-iron complexes were examined using SEM (Hitachi S4800, Japan). Gold was deposited onto the sample surface, and observations were made under high vacuum conditions at an acceleration voltage of 3 kV.

2.5.4.Thermogravimetric analysis (TGA)

The thermal stability of the composite was evaluated using differential scanning calorimetry (DSC, Hitachi TGDTA7300，Japan). First, 3 g of sample was placed in an aluminum crucible. Then, under nitrogen atmosphere, the test temperature range was set from 30 to 650 °C with a heating rate of 10 °C/min. The nitrogen flow rate was maintained at 1 L/min.

2.5.5.Circular dichroism (CD)

Circular dichroism (CD) spectra were measured at 1 nm intervals from 185 to 1000 nm on a circular dichroism (CD) spectrometer (JASCO J-1500, Japan).

2.5.6.X-ray diffraction (XRD)

The crystal structure of the polysaccharide-iron complex was determined using an XRD powder diffractometer (PANalytical X'pert3, Netherlands) at a 2θ range of 10 to 80 Å, a step size of 2 Å (2θ), and a time of 1 second per step.

2.7. In vivo Anti-IDA Activity

2.7.1. IDA Rat model replication

As shown in the figure. Four-week-old male SD rats were acclimated to standard chow for one week before being randomly assigned to model and control groups. The control group (n = 8) received standard chow, while the remaining rats (n = 48) were fed low-iron chow (iron content <5 ppm) supplemented with tail vein bloodletting twice weekly at 1 ml per session for four consecutive weeks. Environmental conditions were maintained at 20–24°C, 40–60% humidity, and a 12-hour light/dark cycle. Rats had free access to chow and ultrapure water throughout the study. Rats were housed in stainless steel cages to prevent iron contamination. After 4 weeks, blood samples were collected via tail vein puncture. Biochemical parameters were measured, and modeling was considered successful when hemoglobin levels fell below 100 g/L. [26]Subsequently, rats with iron deficiency anemia were randomly divided into the model group (gastrointestinal administration of deionized water), positive control group (gastrointestinal administration of Niferex 13.5 mg/kg/day), PSP group (gastrointestinal administration of PSP 13.5 mg/kg/day), and PSP-Fe high-, medium-, and low-dose groups (gastrointestinal administration of PSP-Fe 7.5 mg/kg/day, 13.5 mg/kg/day, and 27 mg/kg/day, respectively). The control group continued receiving blank feed, while the remaining rats were fed low-iron diets. After 4 weeks of administration, rats were anesthetized with sodium pentobarbital, and blood and tissue samples were collected for subsequent experiments. All animal procedures were approved and conducted by the Animal Ethics Committee of Chengdu University of Traditional Chinese Medicine(2024127).

2.7.2. Hematologic Analysis, Iron Levels, and Oxidative Stress Markers

Whole blood was stored in anticoagulant tubes, and red blood cell parameters were determined using automated hematology analyzers (BC-2800Vet Mindray China). A separate blood sample was placed in a standard tube, allowed to stand, and then centrifuged at 3000 rpm for 10 minutes to obtain serum for measuring serum iron levels (E-BC-K758-M, Elabscience, China). Portions of liver tissue were stored at -80°C for measuring hepatic SOD and MDA levels. Iron levels were measured using a commercial assay kit. (E-BC-K020-M, E-BC-K025-M, Elabscience, China)

2.7.3. Histopathological Analysis

Fresh liver, spleen, and kidney tissues were fixed in 4% paraformaldehyde, stained with hematoxylin and eosin (H&E), and then examined under an inverted microscope (Olympus, Tokyo, Japan). Liver tissue was stained with Prussian blue to detect iron.

2.8. Data Analysis

Data are expressed as mean ± standard deviation and analyzed using SPSS 23.0 software. A t-test was performed for comparisons between two groups. For more than two groups, one-way analysis of variance (ANOVA) was conducted, followed by LSD post hoc tests for pairwise comparisons. $P < 0.05$ indicates a statistically significant difference.

3. Results and discussion

3.1. Chemical Composition Analysis

After extracting crude polysaccharides from Polygonatum using the water extraction and ethanol precipitation method, the polysaccharide fraction PSP1 was obtained via DEAE-52 cellulose ion exchange chromatography with gradient elution (**Figure 2A**). Further purification using Sephadex-G100 (**Figure 2B**) yielded a distinct elution peak, designated as PSP. HPLC analysis revealed PSP consists of fructose (Fru), glucose (Glc), and arabinose (Ara) in a molar ratio of 94.18:5.59:0.23.(**Figure 3A**) The anthrone-sulfuric acid method determined PSP purity at 98.0%.($y = 41.011x - 0.0062$ $R^2 = 0.9938$). The same method measured PSP-Fe polysaccharide content at 80.3%, significantly lower than PSP. Preliminary speculation suggests iron ion complexation within the polysaccharide may cause this

purity reduction. This is further evidenced by the color difference: PSP appears white (**Figure 2C**), while PSP-Fe (**Figure 2D**) turns reddish-brown.

The o-phenanthroline method determined the iron content of PSP-Fe to be approximately 20.31%($y=10.463x + 0.0029$ $R^2 = 0.9998$), lower than that of Ziziphus jujuba polysaccharides and Poria cocos polysaccharide-iron complexes[27][28]. The differing capacities of various polysaccharides to bind iron ions may stem from variations in monosaccharide composition and molecular weight among plant polysaccharides. Polysaccharides containing more hydroxyl and carboxyl groups possess greater iron-binding sites.

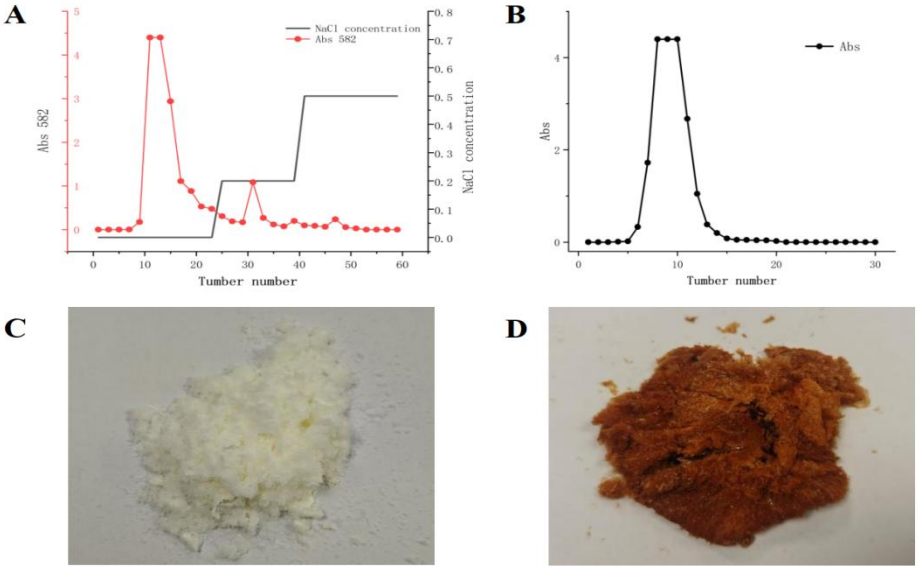

Figure 2. The elution curves of polysaccharides on DEAE and gel and the sample plots of PSP and PSP-Fe were shown. (A), Elution curve of PSP on a DEAE-52 ion exchange column. Elution buffer: water, NaCl (0.2, 0.5 mol/L). Flow rate: 1.0 mL/min (10 min/tube).(**B**), Elution curve of PSP on a dextran gel G-100 column. Elution buffer: water; flow rate: 1.0 mL/min (10 mL/tube). **C**), Polymeric PSP after overgelation. (**D**), PSP-Fe complex.

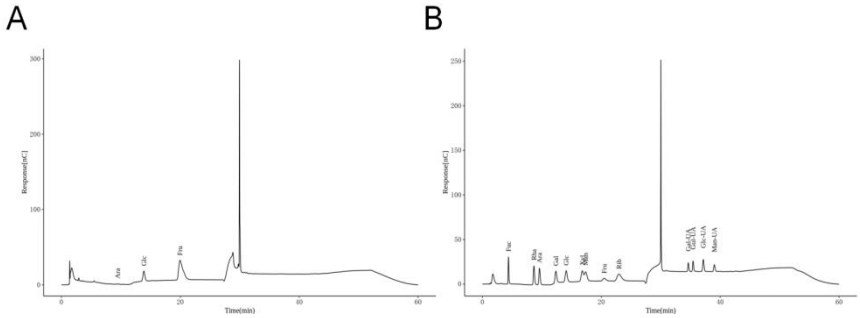

Figure 3. HPLC chromatogram of PSP.

3.2.UV Analysis

As shown in the (Figure 4A), PSP contains trace amounts of protein or nucleic acids, evidenced by faint absorption peaks near 260 and 280 nm. In contrast, the PSP-Fe(III) complex contains almost no protein or nucleic acids, suggesting they may have degraded under the harsh reaction conditions during synthesis. In contrast, the PSP-Fe(III) complex exhibits distinct peaks across the 200–400 nm range, likely due to electron transfer from PSP to Fe^{3+} in the ultraviolet region[29]

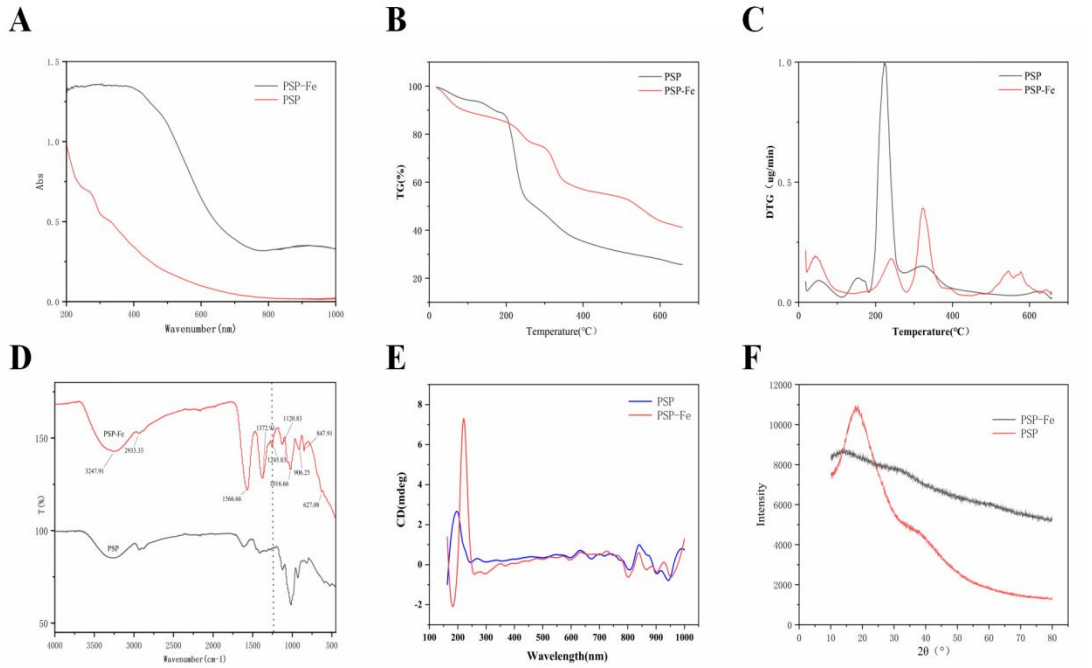

Figure 4. Structural characterization of PSP-Fe.(A-F) represent the UV, TG, DTG, FIR, CD, and XRD spectra of PSP and PSP-Fe, respectively

3.3. FTIR analysis

FTIR serves as a vital tool for analyzing functional groups, offering simplicity and selectivity in the qualitative analysis of compounds. As shown in the (**Figure 4D**), PSP and the PSP-Fe complex exhibit absorption peaks at 3240 cm^{-1} (-OH stretching vibration), 2930 cm^{-1} (C-H bond stretching vibration), Absorption peaks at 1566 cm−1 (C=O stretching vibration) and 1372 cm−1 (O-H bending vibration) are observed. The absorption peak at 1085 cm−1 originates from C-O stretching vibration. The PSP-Fe(III) complex exhibits characteristic absorption peaks of polysaccharides,

broadly resembling the spectrum of PSP, indicating that Fe3+ binding to PSP does not disrupt its active functional groups[30]. However, several spectral peaks exhibited notable changes. Enhanced signal intensity near 3450 cm−1 indicates O-H participation from hydroxyl groups, suggesting Fe3+ may bind PSP via hydroxyl interactions. Significant increases in absorption intensity at 1600 cm−1 and 1420 cm−1 can also be attributed to hydrogen bonding interactions between PSP and Fe3+. The characteristic absorption signal in the β-Fe(III) complex is identified at 850 cm^{-1}[31]. These changes confirm the effective complexation between PSP and Fe^{3+}.

3.4. SEM-EDS Analysis

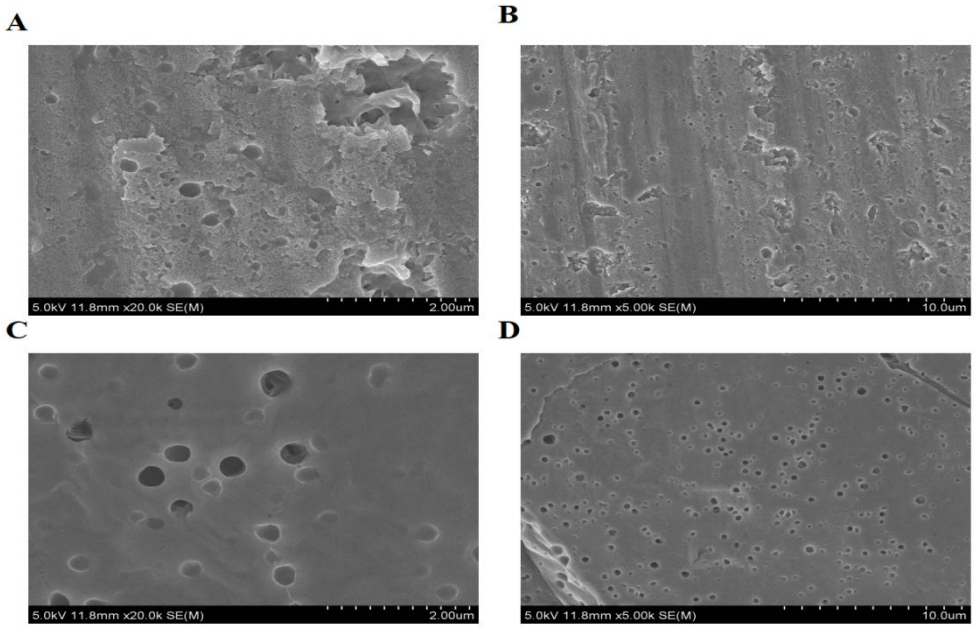

Figure 5. Scanning electron micrographs of PSP-Fe and PSP.(**A, B**) represent the surface morphology of PSP, (**C,D)** represent the surface morphology of PSP-Fe.

The show scanning electron microscope images of PSP **(Figure 5C, D)** and PSP-Fe(III)(**Figure 5A, B)** at magnifications of 5.0K×and 20.0K×, respectively. As shown, PSP exhibits a cohesive morphology characterized by circular, pore-like cavities and an uneven surface. In contrast, as depicted, the PSP-Fe(III) complex displays a markedly smoother surface. This phenomenon can be attributed to coordination between polysaccharides and iron ions, molecular cross-linking, and conformational changes within the polysaccharides[31].

As shown in the (**Figure 6A-D**), the surface elemental composition of the PSP-Fe(III) complex is: Fe (23.55%), C (23.73%), O (52.73%), while PSP consists of C (45.66%), O (54.30%), and Fe (0.04%). In summary, PSP formed a complex with Fe^{3+}, successfully yielding a polysaccharide-iron complex.

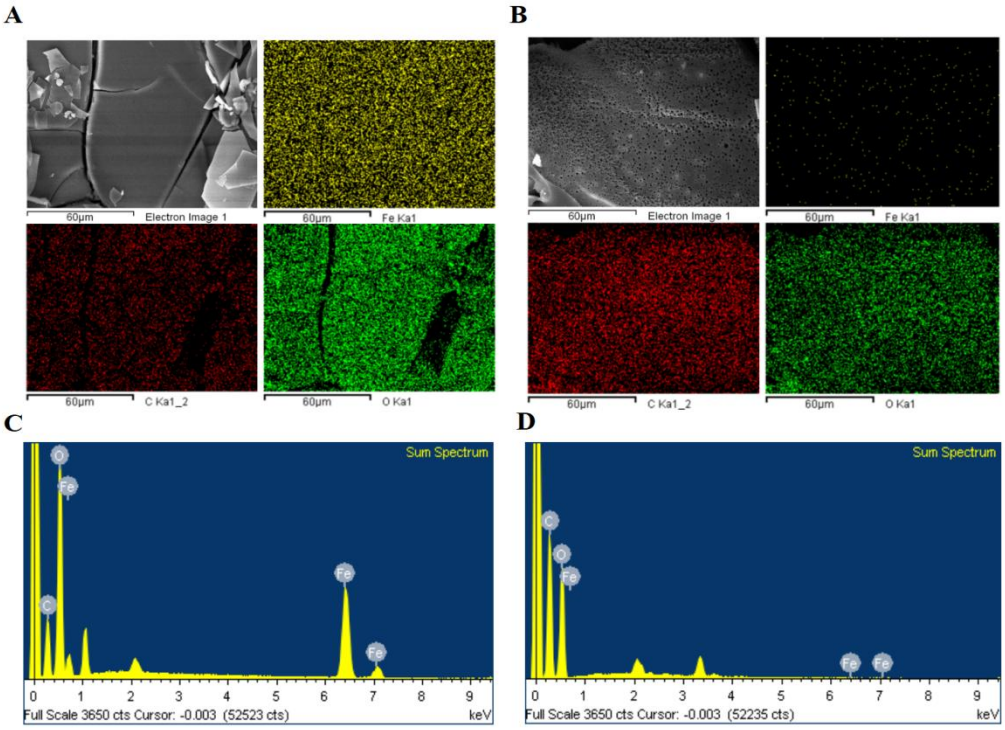

Figure 6. Surface element distribution of PSP-Fe and PSP.(**A, C**) show the surface element distribution of PSP-Fe, while (**B, D**) show the surface

3.5. Thermal Stability Analysis

As an excellent iron supplement, polysaccharide-iron complexes require high stability during production, storage, and transportation. Insufficient stability may lead to structural instability and compromise the intended iron supplementation efficacy. The thermal stability of PSP and PSP-Fe(III) complexes was evaluated using thermogravimetric analysis (TG) and differential thermogravimetric analysis (DTG). The complexation of Fe^{3+} altered the thermodynamic behavior of the polysaccharide. In the TG profiles (**Figure 4B**), he thermal decomposition of both PSP and PSP-Fe(III) complexes was divided into three stages: the first stage occurred in the temperature range of 18.10–224.53°C for the PSP-Fe(III) complex and 18.10–197.81°C for PSP (attributed to the loss of moisture and volatile compounds). The second stage occurred between 224.53–501.67°C and 197.8–502.96°C (maximum mass loss of 47.54% and 69.41% due to decarboxylation and thermal decomposition, respectively). The third stage occurred between 510.25–650.15°C (carbonization stage). The increase in

residual mass observed at the end of each stage indicates enhanced thermal stability of the PSP-Fe(III) complex. In the DTG curve (**Figure 4C**) the first endothermic peak of PSP appeared earlier (223.89°C, 0.99 μg/min) and reached the maximum decomposition rate before that of the PSP-Fe(III) complex. The maximum decomposition rate of the PSP-Fe(III) complex was observed at 322.41°C with a rate of 0.39 μg/min. Compared to PSP, the PSP-Fe(III) complex exhibits a lower weight loss rate and higher pyrolysis temperature, indicating superior thermal stability of the polysaccharide-iron complex over the polysaccharide alone. This phenomenon may be attributed to the chelation of iron ions with polysaccharides, which promotes ordered molecular arrangement and enhances complex stability. This finding aligns with previous studies on iron complexes of Astragalus polysaccharides, corn silk polysaccharides, and Spirulina polysaccharides[32]. On the other hand, Fe^{3+} forms stable β-FeOOH iron cores with polar groups on polysaccharides, enhancing the stability of their spatial structure and improving their thermal stability[33].

3.6. XRD Analysis

X-ray diffraction (XRD) is a key analytical technique for studying the crystal structure of polysaccharides[34]. Due to differences in chemical composition and structural parameters among various substances, distinct diffraction patterns emerge when X-rays pass through crystals, serving as critical indicators for identifying material structures. As shown in the (**Figure 4F**) , PSP exhibits a distinct characteristic peak at 2θ = 20, indicating its amorphous structure. The X-ray diffraction peak at 2θ = 20 disappears in the PSP-Fe(III) complex, likely due to the introduction of Fe^{3+} weakening hydrogen bonding interactions, increasing steric barriers, and reducing group concentration[35].In addition, new faint diffraction peaks characteristic of iron appear at 35°and 60°in the polysaccharide-iron complex[36]. Results indicate that the interaction between PSP and Fe^{3+} leads to a decrease in the crystallinity of the PSP-Fe(III) complex, further validating the successful chelation of PSP with Fe^{3+}. Additionally, no additional characteristic peaks were observed in the X-ray diffraction spectrum of PSP-Fe(III), suggesting that the complex may possess an amorphous structure, potentially exhibiting excellent solubility and bioavailability.

3.7. CD Analysis

Circular dichroism (CD), an effective technique to investigate the three-dimensional structure, was used to compare the difference between the conformation of PSP and PSP-Fe(III) in the present study. As shown in (**Figure 4E**), the peak of PSP near 200 nm mainly comes from the n → σ or π → π transitions of C = O, C-O-C and other groups of the sugar ring. The peak of PSP-Fe (III) at 230 nm may be the d → d transition or charge transfer transition (LMCT) generated by the coordination of metal ions with polysaccharide ligands, and the transition is in a chiral environment, showing obvious Cotton effect in the CD spectrum. Similar phenomena have also been reported in CAP[27] and AGSP[36]. The Cotton peak near 230 nm is often used as a marker of complex formation. At the same time, combined with the UV spectrum (**Figure 4A**), the complex has a weak wide absorption at 300-350 nm, which further supports the existence of Fe-O-Fe bridging or multinuclear coordination.

3.8. Effects of PSP-Fe(III) Complex on IDA Rats

3.8.1. Effects of IDA on Growth and Development in Rats

Changes in rat body weight during modeling are shown in **Table 2**. Starting from the third week, significant differences ($p < 0.05$) emerged between all model groups and the normal control group. After 4 weeks of treatment following randomization, body weight differences were significant ($p < 0.05$) between all treatment groups and the IDA group, except for the PSP group. Rats in all groups exhibited rapid weight gain, showing no significant difference ($p > 0.05$) compared to the normal group (**Figure 7B**）.

Table 1. Red blood cell parameters of rats in each group after modeling

Group	HGB(g/L)	RBC(10^{12}/L)	HCT(%)	MCV(fL)	MCH(pg)	MCHC(g/L)	RDW(%)
NC	158±5	7.65±0.48	47.1±1.9	61.6±1.8	21±1	335.3±10.1	15.49±1.03
Model1	101±21*	6.76±1.13	29.7±6.2*	43.7±2.4*	15±1*	339.1±12.2	31.81±3.35*
Model2	94±9*	5.08±0.85*	30.1±5.6*	59.3±2.4#	19±2*	315.0±30.8	20.26±1.87*
Model3	100±10*	7.23±0.89	30.3±3.8*	42.0±1.7*	14±1*	331.0±13.3	28.20±3.10*
Model4	99±11*	6.99±0.52	29.2±3.4*	41.8±2.1*	14±1*	337.1±5.2	29.35±3.53*
Model5	95±14*	5.94±1.29*	36.2±5.7*	63.7±3.6	17±3*	267.5±53.4*	20.81±3.01*
Model6	84±10*	6.17±0.98*	25.3±3.9*	41.0±1.4*	14±1*	335.6±18.3	31.05±2.42*

Note: Indicates a statistically significant difference compared to the control group(p*<0.*05)*.

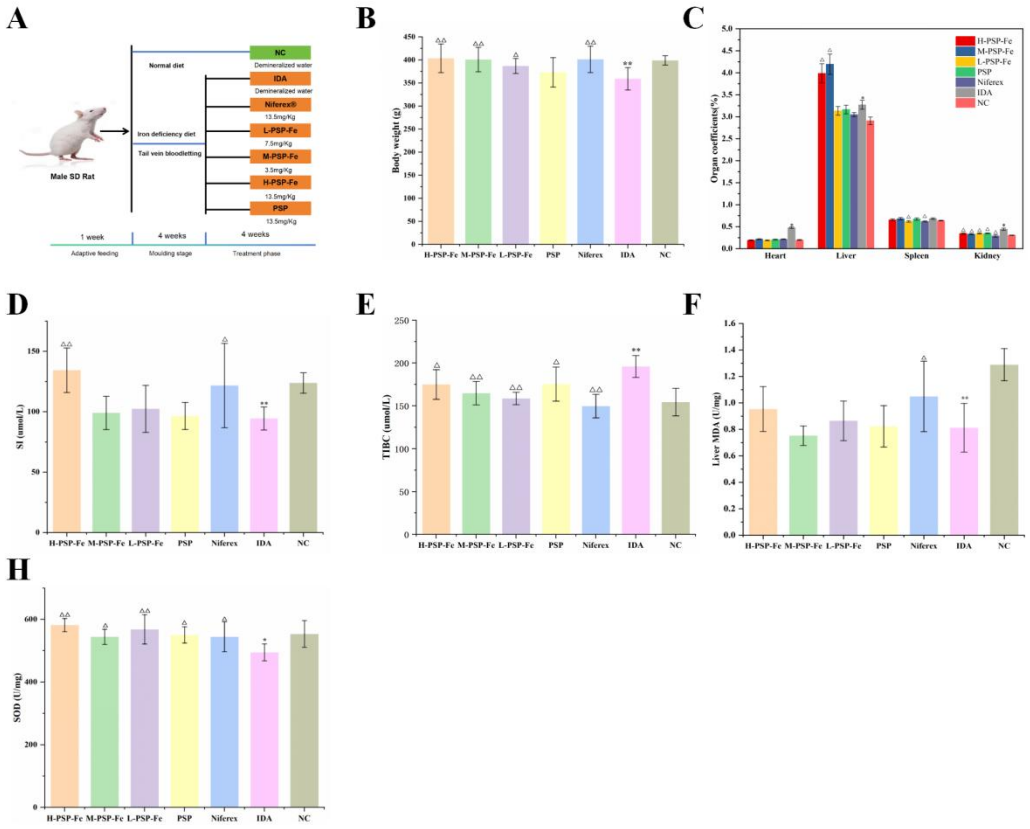

Figure 7.(**A**), Animal experiment design, (**B**), Differences in rat body weight at the end of the experiment, (**C**) , heart, liver, spleen, and kidney coefficients. Values were presented as the mean ± SE (n =8),(**D**), serum iron,(**E**), Total iron binding capacity,(**F**) Liver SOD,(**G**), Liver MDA

Organ coefficients, serving as indicators of drug safety, are commonly used to assess drug toxicity. As shown in cardiac, hepatic, splenic, and renal coefficients were calculated for each group post-sacrifice. Compared to the NC group, both cardiac and splenic coefficients were significantly increased in the IDA group ($P < 0.05$). This may indicate that under the influence of IDA or related diseases, the spleen continuously undergoes hematopoietic tissue regeneration, leading to splenomegaly[37]. of the cardiac oblique sinus, red blood cell aggregation, and compensatory cardiac blood supply are associated with increased myocardial cell volume[38]. with the NC group, the liver and kidney coefficients were significantly reduced in IDA rats ($P < 0.05$). In the H-CAP-Fe(III) group, the heart and spleen coefficients were significantly reduced, while the kidney coefficient was significantly increased. The reduction in liver volume may be attributed to decreased hepatocyte

size and organelle volume. In summary, the PSP-Fe(III) complex can positively influence the health of IDA mice.

Table 2. Changes in Rat Body Weight During Modeling Period

Group	Week 1(g)	Week 2(g)	Week 3(g)	Week 4(g)
NC	140.35±7.35	176.15±13.79	244.89±10.72	301.94±18.05
Model1	133.59±5.71	170.43±6.75	218.95±9.96*	266.77±12.99*
Model2	141.43±6.48	168.48±12.90	207.07±17.24*	241.68±34.09*
Model3	136.12±4.93	167.44±11.10	206.49±12.08*	241.94±15.83*
Model4	144.65±5.34	167.43±7.45	218.96±14.29*	252.03±21.63*
Model5	141.91±6.10	172.32±9.24	206.19±17.00*	249.48±22.96*
Model6	140.76±3.51	173.76±9.75	211.17±13.66*	248.71±16.59*

Note: Indicates a statistically significant difference compared to the control group(p*<0.05).

Table 3. Hemoglobin parameters in rats from each group after treatment

Group	HGB(g/L)	RBC(10^{12}/L)	HCT(%)	MCV(fL)	MCH(pg)	MCHC(g/L)	RDW(%)
H-PSP-Fe	165±11$^{\triangle\triangle}$	8.64±0.57$^{\triangle\triangle}$	49.5±3.7$^{\triangle\triangle}$	57.3±2.6$^{\triangle\triangle}$	19±1.0	334.7±5.9$^{\triangle\triangle}$	15.12±0.88$^{\triangle\triangle}$
M-PSP-Fe	147±5$^{\triangle\triangle}$	8.33±1.26$^{\triangle\triangle}$	43.2±1.5$^{\triangle\triangle}$	52.7±6.1$^{\triangle\triangle}$	17±2.4	341.0±8.9$^{\triangle\triangle}$	24.95±3.19$^{\triangle\triangle}$
L-PSP-Fe	135±14$^{\triangle\triangle}$	9.72±0.62$^{\triangle\triangle}$	39.6±3.8$^{\triangle\triangle}$	40.8±2.8	14±1.2$^{\triangle\triangle}$	339.3±5.3$^{\triangle\triangle}$	25.66±2.32$^{\triangle}$
PSP	113±21	8.00±3.01	31.7±11.1$^{\triangle\triangle}$	40.7±5.4	16±6.2	390.0±113.3	27.34±3.56
Niferx	150±20$^{\triangle\triangle}$	9.35±1.05$^{\triangle\triangle}$	46.1±6.9$^{\triangle\triangle}$	49.3±5.4$^{\triangle\triangle}$	16±1.8	328.3±28.1$^{\triangle\triangle}$	23.25±4.55$^{\triangle\triangle}$
IDA	77±22**	4.20±1.80**	17.0±5.6**	42.2±4.9**	21±7.3*	479.4±129.4**	29.69±2.45**
NC	175±9	8.73±0.15	51.5±3.2	58.9±13	20±0.5	339.9±5.9	12.99±0.57

Note: *P < 0.05,**P < 0.01 compared to normal group. $^{\triangle}$P < 0.05, $^{\triangle\triangle}$P < 0.01 compared to model group.

3.8.2. Effects on Red Blood Cell Parameters

As shown in **Table 1** , after four weeks of modeling, the IDA group exhibited significantly lower red blood cell count (RBC), hemoglobin (HGB), hematocrit (HCT), mean corpuscular hemoglobin (MCH), and mean corpuscular volume (MCV) compared to the NC group, while the red cell distribution width (RDW) was significantly higher ($p < 0.05$), indicating that iron deficiency impaired hematopoietic function.As shown in **Table 3**,Following supplementation with PSP-Fe(III) complex, IDA rats exhibited significant increases in RBC, HGB, HCT, MCH, mean corpuscular hemoglobin concentration (MCHC), and mean corpuscular volume (MCV), while RDW decreased to normal levels ($p < 0.05$). This demonstrates that PSP-Fe(III) significantly improves various blood parameters in iron-deficient anemic rats, thereby

alleviating iron deficiency. It demonstrates great potential and application value in treating iron deficiency anemia and as an iron supplement.

Serum iron (SI) content reflects iron bound to transferrin in serum, while total iron-binding capacity (TIBC) indicates the maximum iron capacity bound to all transferrin in serum, serving as crucial indicators for assessing human iron metabolism. Figure 7D and Figure 7E demonstrate that serum iron levels in the H-PSP-Fe(III) and Niferex groups were significantly elevated ($P < 0.05$) compared to the IDA group. Conversely, the figure indicates significantly reduced TIBC levels in the Niferex, M-PSP-Fe, and H-PSP-Fe groups. In summary, Niferex and PSP-Fe groups effectively restored serum iron and TIBC levels, consistent with reports on oyster protein hydrolysate iron complexes[39]. ameliorates hypoferremia symptoms caused by iron deficiency anemia ($P < 0.05$).

3.8.3.Effect of PSP-Fe (III) complex on oxidative stress

Excessive or deficient iron levels in the body can alter the activity of certain antioxidant enzymes. **Figure 7D-F** indicate that long-term low-iron diets lead to significant oxidative imbalance, as evidenced by elevated MDA levels observed in the IDA group ($P < 0.05$). The H-PSP-Fe group significantly reduced MDA content. As shown in **Figure 7F-G** after 4 weeks of continuous treatment, PSP-Fe significantly increased SOD activity and decreased MDA content in the liver ($P < 0.05$). Results indicate that PSP-Fe(III) ameliorates IDA-induced oxidative stress more effectively than the Niferex group.

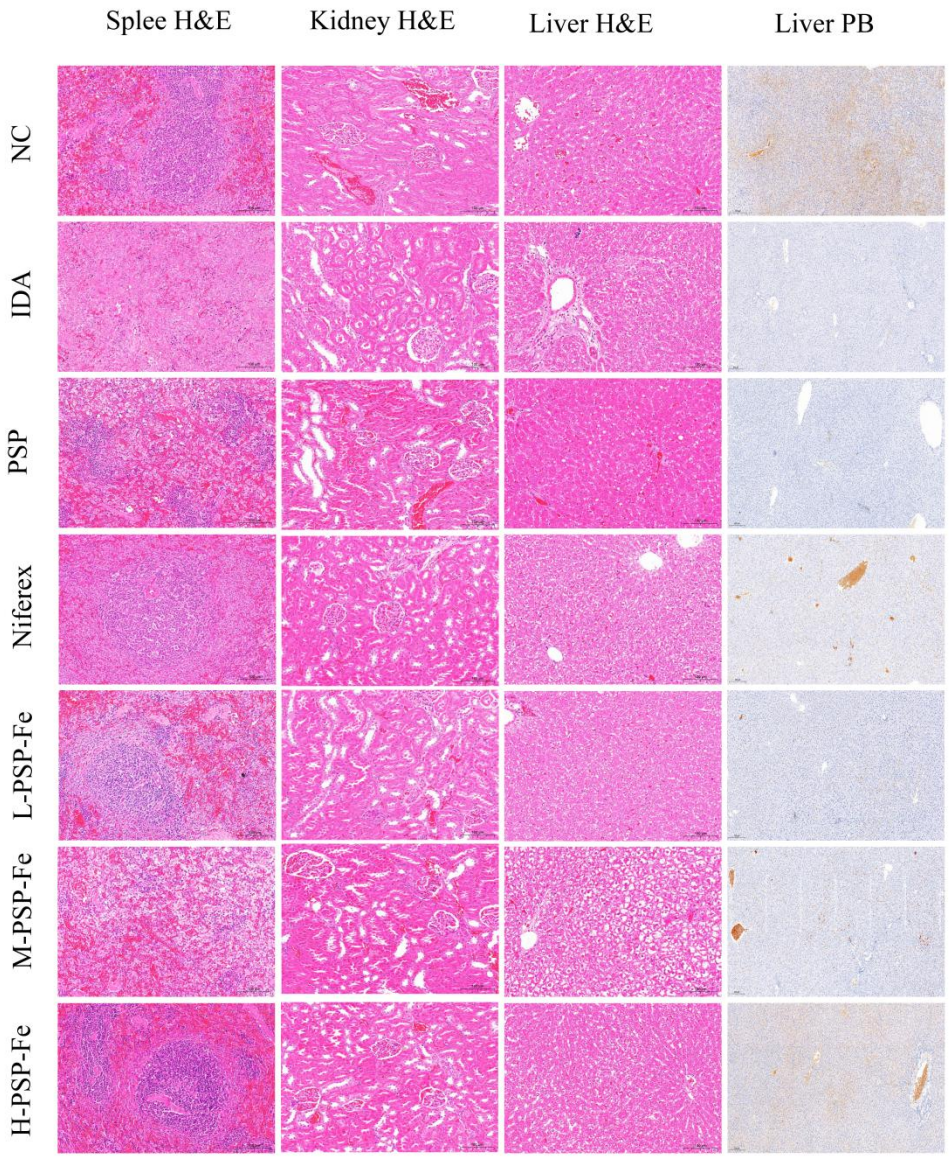

Figure 8. Histological analysis of the effect of PSP-Fe (III) on IDA rats

3.8.4. Histopathological analysis

In the **Figure 8**, the IDA group exhibits irregularly arranged and mildly enlarged hepatic sinusoids in liver tissue, accompanied by marked splenic and inflammatory lesions, such as the presence of macrophages and inflammatory cells, as well as localized tubular damage. After 4 weeks of treatment, PSP-Fe(III) reduced tissue damage in the liver, spleen, and kidneys, indicating its favorable biosafety profile. Prussian blue staining was used to reflect iron levels in organs. Iron-containing areas appear brown, with darker shades indicating higher iron content. As shown, liver iron content was higher around the central vein in the NC group, while the IDA group

exhibited lower levels. Both the M-PSP-Fe and H-PSP-Fe groups showed significant improvement compared to the IDA group. Conclusion: PSP-Fe(III) exhibits a pronounced iron-supplementing effect in IDA mice.

4.Conclusions

This study successfully isolated PSP polysaccharide from Polygonatum through systematic extraction, separation, and purification techniques. The polysaccharide content was measured at 98.0%, composed of monosaccharides fructose (Fru), glucose (Glc), and arabinose (Ara) with a molar ratio of 94.18:5.59:0.23. Furthermore, the PSP-Fe(III) complex was synthesized, and its chemical composition, structural characterization, and protective effects on iron-deficient anemic rats were investigated. Overall, the iron content of the PSP-Fe(III) complex was 22.31%. The structure of the β-Fe(III) complex was confirmed through infrared spectroscopy and X-ray diffraction analysis. Furthermore, the complexation of PSP with Fe^{3+} conferred higher thermal stability to the complex, reduced its crystallinity, and altered its morphological characteristics. In animal experiments, PSP-Fe(III) improved growth and development, red blood cell parameters, iron status indices, oxidative stress levels, and tissue morphology in iron-deficient anemic rats. In summary, the PSP-Fe(III) complex may serve as an effective iron supplement for treating iron-deficiency anemia. Furthermore, the complex structure of the polysaccharide-iron complex warrants subsequent investigation using more advanced techniques and research methods to elucidate its molecular architecture. Concurrently, its toxicity, clinical applications, iron release mechanisms, and regulatory effects on iron metabolism require further exploration.

Funding: This work was funded by the Key Project of the Sichuan Science and Technology Department (no. 2021YFN0015 and 2022YFS0444), the Project of Sichuan Traditional Chinese MedicineAdministration (no. 2023MS432), and the Chengdu Science and Technology Bureau TechnologyInnovation Research and Development Project (no. 2021-YF05-02298-SN).

References

[1] The Chinese Pharmacopoeia; Chinese Medicine Publishing House: Beijing, China, 2020.
[2] Zhao, P., Li, X., Wang, Y., Yan, L., Guo, L., Huang, L., & Gao, W. (2020). Characterisation and saccharide mapping of polysaccharides from four common Polygonatum spp. Carbohydrate polymers, 233, 115836. https://doi.org/10.1016/j.carbpol.2020.115836
[3] Zhao, P., Li, X., Wang, Y., Zhang, X., Jia, H., Guo, L., Huang, L., & Gao, W. (2020). Comparative studies on characterization, saccharide mapping and antiglycation activity of polysaccharides from different Polygonatum ssp. Journal of pharmaceutical and biomedical analysis, 186, 113243. https://doi.org/10.1016/j.jpba.2020.113243
[4] Cui, X., Wang, S., Cao, H., Guo, H., Li, Y., Xu, F., Zheng, M., Xi, X., & Han, C. (2018). A Review: The Bioactivities and Pharmacological Applications of Polygonatum sibiricum polysaccharides. Molecules (Basel, Switzerland), 23(5), 1170. https://doi.org/10.3390/molecules23051170
[5] Domenech, J., Barasoain, I., Prieto, A., Gómez-Miranda, B., Bernabé, M., & Leal, J. A. (1996). An antigenic water-soluble glucogalactomannan extracted from cell walls of Paecilomyces fumosoroseus and Paecilomyces farinosus. Microbiology (Reading, England), 142 (Pt 12), 3497–3503. https://doi.org/10.1099/13500872-142-12-3497
[6] Yelithao, K., Surayot, U., Lee, J. H., & You, S. (2016). RAW264.7 Cell Activating Glucomannans Extracted from Rhizome of Polygonatum sibiricum. Preventive nutrition and food science, 21(3), 245–254. https://doi.org/10.3746/pnf.2016.21.3.245
[7] Li, X., Chen, Q., Liu, G., Xu, H., & Zhang, X. (2021). Chemical elucidation of an arabinogalactan from rhizome of Polygonatum sibiricum with antioxidant activities. International journal of biological macromolecules, 190, 730–738. https://doi.org/10.1016/j.ijbiomac.2021.09.038
[8] Zhao, J., Ma, L., Ni, Z., & Liu, H. (2021). In vitro facilitating role of polygonatum sibiricum polysaccharide in osteogenic differentiation of bone marrow mesenchymal stem cells from patients with multiple myeloma. Biotechnology letters, 43(7), 1311–1322. https://doi.org/10.1007/s10529-021-03125-x
[9] Liu, B., Tang, Y., Song, Z., & Ge, J. (2021). Polygonatum sibiricum F. Delaroche polysaccharide ameliorates HFD- induced mouse obesity via regulation of lipid metabolism and inflammatory response. Molecular medicine reports, 24(1), 501. https://doi.org/10.3892/mmr.2021.12140
[10] Wang, Y., Lan, C., Liao, X., Chen, D., Song, W., & Zhang, Q. (2019). Polygonatum sibiricum polysaccharide potentially attenuates diabetic retinal injury in a diabetic rat model. Journal of diabetes investigation, 10(4), 915–924. https://doi.org/10.1111/jdi.12976
[11] Li, Q., Zeng, J., Gong, P., Wu, Y., & Li, H. (2021). Effect of steaming process on the structural characteristics and antioxidant activities of polysaccharides from Polygonatum sibiricum rhizomes. Glycoconjugate journal, 38(5), 561–572. https://doi.org/10.1007/s10719-021-10013-z
[12] Shen, F., Song, Z., Xie, P., Li, L., Wang, B., Peng, D., & Zhu, G. (2021). Polygonatum sibiricum polysaccharide prevents depression-like behaviors by reducing oxidative

stress, inflammation, and cellular and synaptic damage. Journal of ethnopharmacology, 275, 114164. https://doi.org/10.1016/j.jep.2021.114164

[13] Al Hassan N. N. (2015). The prevalence of iron deficiency anemia in a Saudi University female students. Journal of microscopy and ultrastructure, 3(1), 25–28. https://doi.org/10.1016/j.jmau.2014.11.003

[14] Cappellini, M. D., Musallam, K. M., & Taher, A. T. (2020). Iron deficiency anaemia revisited. Journal of internal medicine, 287(2), 153–170. https://doi.org/10.1111/joim.13004

[15] Cottin, S. C., Gambling, L., Hayes, H. E., Stevens, V. J., & McArdle, H. J. (2016). Pregnancy and maternal iron deficiency stimulate hepatic CRBPII expression in rats. The Journal of nutritional biochemistry, 32, 55–63. https://doi.org/10.1016/j.jnutbio.2016.02.005

[16] Denic, S., & Agarwal, M. M. (2007). Nutritional iron deficiency: an evolutionary perspective. Nutrition (Burbank, Los Angeles County, Calif.), 23(7-8), 603–614. https://doi.org/10.1016/j.nut.2007.05.002

[17] Oshtrakh, M. I., Milder, O. B., & Semionkin, V. A. (2006). Determination of the iron state in ferrous iron containing vitamins and dietary supplements: application of Mössbauer spectroscopy. Journal of pharmaceutical and biomedical analysis, 40(5), 1281–1287. https://doi.org/10.1016/j.jpba.2005.09.020

[18] Ren F, Qian XH, Qian XL. (2016).Astragalus polysaccharide upregulates hepcidin and reduces iron overload in mice via activation of p38 mitogen-activated protein kinase. Biochemical and Biophysical Research Communications. 2016 Mar;472(1):163-168. https://doi.org/10.1016/j.bbrc.2016.02.088.

[19] Zhang, Z. S., Wang, X. M., Han, Z. P., Yin, L., Zhao, M. X., & Yu, S. C. (2012). Physicochemical properties and inhibition effect on iron deficiency anemia of a novel polysaccharide-iron complex (LPPC). Bioorganic & medicinal chemistry letters, 22(1), 489–492. https://doi.org/10.1016/j.bmcl.2011.10.100

[20] Tahir, A., & Khan, A. Q. (2025). Exploring the Potential of Machine Learning and Deep Learning for Predictive Breast Cancer Analytics. ICCK Transactions on Radiology and Imaging, 1(1), 11–42. https://doi.org/10.62762/TRI.2025.234235

[21] Zheng, J., Yue, X., Dai, Z., Wang, Y., Liu, S., & Yan, X. (2009). Novel iron-polysaccharide multilayered microcapsules for controlled insulin release. Acta biomaterialia, 5(5), 1499–1507. https://doi.org/10.1016/j.actbio.2009.01.017

[22] Zhang, Y. Y., Liu, J. H., Su, F., Lui, Y. T., & Li, J. F. (2009). Single-dose bioequivalence assessment of two formulations of polysaccharide iron complex capsules in healthy adult male Chinese volunteers: A sequence-randomized, double-blind, two-way crossover study. Current therapeutic research, clinical and experimental, 70(2), 104–115. https://doi.org/10.1016/j.curtheres.2009.04.006

[23] Viteri, F. E., Casanueva, E., Tolentino, M. C., Díaz-Francés, J., & Erazo, A. B. (2012). Antenatal iron supplements consumed daily produce oxidative stress in contrast to weekly supplementation in Mexican non-anemic women. Reproductive toxicology (Elmsford, N.Y.), 34(1), 125–132. https://doi.org/10.1016/j.reprotox.2012.03.010

[24] Liu, M., Wang, Y., Wang, R., Zong, W., Zhang, L., & Wang, L. (2024). Preparation and Performance Evaluation of Polysaccharide-Iron Complex of Eucommia

ulmoides. Foods (Basel, Switzerland), 13(14), 2302. https://doi.org/10.3390/foods13142302

[25] Zhang, X., Zhang, X., Gu, S., Pan, L., Sun, H., Gong, E., Zhu, Z., Wen, T., Daba, G. M., & Elkhateeb, W. A. (2021). Structure analysis and antioxidant activity of polysaccharide-iron (III) from Cordyceps militaris mycelia. International journal of biological macromolecules, 178, 170–179. https://doi.org/10.1016/j.ijbiomac.2021.02.163

[26] Cui, J., Li, Y., Yu, P., Zhan, Q., Wang, J., Chi, Y., & Wang, P. (2018). A novel low molecular weight Enteromorpha polysaccharide-iron (III) complex and its effect on rats with iron deficiency anemia (IDA). International journal of biological macromolecules, 108, 412–418. https://doi.org/10.1016/j.ijbiomac.2017.12.033

[27] Xie, J., Wu, N., Li, D., Xiong, S., Dong, J., Wang, R., Zheng, G., & Li, J. (2025). Characterization of Choerospondias axillaris polysaccharide- iron (III) complex and its effect on iron deficiency anemia mice. International journal of biological macromolecules, 296, 139759. https://doi.org/10.1016/j.ijbiomac.2025.139759

[28] Zhang, Y., Huang, J., Sun, M., Duan, Y., Wang, L., Yu, N., Peng, D., Chen, W., & Wang, Y. (2023). Preparation, characterization, antioxidant and antianemia activities of Poria cocos polysaccharide iron (III) complex. Heliyon, 9(1), e12819. https://doi.org/10.1016/j.heliyon.2023.e12819

[29] Gao, W., Huang, Y., He, R., & Zeng, X. A. (2018). Synthesis and characterization of a new soluble soybean polysaccharide-iron(III) complex using ion exchange column. International journal of biological macromolecules, 108, 1242–1247. https://doi.org/10.1016/j.ijbiomac.2017.11.038

[30] Zhang, X., Zhang, X., Gu, S., Pan, L., Sun, H., Gong, E., Zhu, Z., Wen, T., Daba, G. M., & Elkhateeb, W. A. (2021). Structure analysis and antioxidant activity of polysaccharide-iron (III) from Cordyceps militaris mycelia. International journal of biological macromolecules, 178, 170–179. https://doi.org/10.1016/j.ijbiomac.2021.02.163

[31] Wang, J., Chen, H., Wang, Y., & Xing, L. (2015). Synthesis and characterization of a new Inonotus obliquus polysaccharide-iron(III) complex. International journal of biological macromolecules, 75, 210–217. https://doi.org/10.1016/j.ijbiomac.2015.01.041

[32] Jia, N., Qiao, H., Zhu, W., Zhu, M., Meng, Q., Lu, Q., & Zu, Y. (2019). Antioxidant, immunomodulatory, oxidative stress inhibitory and iron supplementation effect of Astragalus membranaceus polysaccharide-iron (III) complex on iron-deficiency anemia mouse model. International journal of biological macromolecules, 132, 213–221. https://doi.org/10.1016/j.ijbiomac.2019.03.196

[33] Liu, M., Wang, Y., Wang, R., Zong, W., Zhang, L., & Wang, L. (2024). Preparation and Performance Evaluation of Polysaccharide-Iron Complex of Eucommia ulmoides. Foods (Basel, Switzerland), 13(14), 2302. https://doi.org/10.3390/foods13142302

[34] Evans, P., Rogers, K., Dicken, A., Godber, S., & Prokopiou, D. (2014). X-ray diffraction tomography employing an annular beam. Optics express, 22(10), 11930–11944. https://doi.org/10.1364/OE.22.011930

[35] Lazaridis, N. K., Kyzas, G. Z., Vassiliou, A. A., & Bikiaris, D. N. (2007). Chitosan derivatives as biosorbents for basic dyes. Langmuir : the ACS journal of surfaces and colloids, 23(14), 7634–7643. https://doi.org/10.1021/la700423j

[36] Wang, L., Wang, L., Su, C., Wen, C., Gong, Y., You, Y., Zhao, J., Han, Y., Song, S., & Xiao, H. (2020). Characterization and digestion features of a novel polysaccharide-Fe(III) complex as an iron supplement. Carbohydrate polymers, 249, 116812. https://doi.org/10.1016/j.carbpol.2020.116812

[37] Wei, Y. H., He, Y. Z., Guo, X. Y., Lin, X. Y., Zhu, H. B., & Guo, X. J. (2021). Investigation and Analysis of Iron-Deficiency Anemia Complicated by Splenomegaly. International journal of general medicine, 14, 4155–4159. https://doi.org/10.2147/IJGM.S324164

[38] Tang, N., Chen, L. Q., & Zhuang, H. (2014). Effects of heme iron enriched peptide on iron deficiency anemia in rats. Food & function, 5(2), 390–399. https://doi.org/10.1039/c3fo60292c

[39] Liu, X., Yu, X., Dou, S., Yin, F., Li, D., & Zhou, D. (2023). Characterization of Oyster Protein Hydrolysate-Iron Complexes and their In Vivo Protective Effects against Iron Deficiency-Induced Symptoms in Mice. Journal of agricultural and food chemistry, 71(44), 16618–16629. https://doi.org/10.1021/acs.jafc.3c05182